International Journal of Engineering

Journal Homepage: www.ije.ir

Determination of Blast Impact Range and Safe Distance for a Reinforced Concrete Pile Under Blast Loading

M. Khodaparast*, S. H. Hosseini, H. Moghtadaei

Faculty of Engineering, University of Qom, Qom, Iran

A B S T R A C T

Piles transfer structural loads to the hard layers of the soil or rock; thus, any damage to the pile foundations could have irreparable consequences. A surface blast can create a ground shock that transmits the blast energy along the surface and at depths. Explosion research necessitates technical design to mitigate the adverse effects on nearby structures and facilities. The blast impact range and the safe distance at which the pile will avoid structural damage are two critical parameters for the design of a pile under blast loading. Therefore, this study used the coupled Eulerian-Lagrangian method to determine the blast impact range and safe distance for reinforced concrete piles (RC piles) subjected to blast loading. The results for clayey and sandy soils revealed that an increase in the explosive depth had no significant effect on the safe distance, despite a decrease in the compressive and tensile damage to the pile. Increasing the mass and depth of the blast decreased the ultimate compressive bearing capacity of the pile and increased the blast impact range. Sandy soil performed better than clayey soil against blast loading. The findings of this study can be applied to various projects, including critical structures near gas transmission lines or vulnerable to terrorist attacks.

doi: 10.5829/ije.2023.36.02b.17

1. INTRODUCTION

Pile foundations are used in civil structures to transfer the structural load to the depth of the soil or rock layers. It is critical to consider soil behavior in dynamic load presence [1, 2]. Any damage to the pile foundations can lead to failure of the structure [3]. The shockwave from a surface explosion will transfer the blast energy along the ground surface and to the underlying layers. One potential source of damage which can lead to failure of a pile from blast loading is an explosion at the surface or in the depths. As a pile collapses under blast loading, the upper structure will become vulnerable and collapse; therefore, it is necessary to evaluate the damage factors in a pile subjected to blast loading [4].

The studies conducted on this subject have used both field and laboratory experiments as well as analytical and numerical methods for their investigations. However, because of the difficulties and security issues associated with field and laboratory experiments, numerical

methods more often are used. Therefore, many numerical studies have been prepared in this field.

Prasanna and Boominathan [5] conducted a numerical study on the factors influencing the response of underground tunnels subjected to internal blasts using the finite element method. They studied the effect of the blast on variables that included the material, thickness and shape of the lining. They also found that box-shaped tunnels were more vulnerable to blasts than horseshoe-shaped and circular tunnels.

Problems related to numerical modeling of the blast load include the large deformation caused by the blast load and consideration of the soil-structure interaction. Qiu et al. [6] applied the coupled Eulerian-Lagrangian method (CEL) to geotechnical problems with large deformations. They found that the CEL method was suitable for solving problems caused by major deformations, such as severe distortion and contact problems. They also found this method suitable for investigation of the soil-structure interaction in

Corresponding Author Institutional Email: khodaparast@qom.ac.ir (M. Khodaparast)

geotechnical problems with large deformations, such as explosions.

Other researchers also have investigated the impact of the blast load on the pile foundations. The behavior of pile foundations in saturated sandy soil under blast loading was investigated by Jayasinghe et al. [7] by considering the soil-pile interaction in FE software using LS-DYNA. They studied the distribution of the blast waves in the soil, vertical deformation of the pile, and effective stresses on the pile. The results showed that the pile head was more vulnerable to blast waves and that the effect of the blast on the pile decreased as the distance between them increased.

Huang et al. [8] developed a numerical dynamic analysis approach in LS-DYNA to evaluate the soil-pile interaction under blast loading. They found that the maximum shear stress on the head of the pile was greater than at the tip and that the stress distribution along the pile length showed an inverted triangular model. They also found that the maximum contact pressure between the soil and pile was concentrated at the pile head.

Jayasinghe et al. [9] studied the blast response of RC piles in saturated sandy soil. They reported that sufficient longitudinal reinforcement and proper detailing of transverse reinforcement could reduce the vulnerability of RC piles.

Chakraborty [10] carried out a numerical study in Abaqus to analyze the performance of a hollow steel pile exposed to an explosion at depth. It was concluded that the lateral deformation increased with an increase in the lateral load. It was also found that, in loose soil, the maximum velocity in the soil particles increased as the elastic modulus, specific gravity, and friction angle decreased.

Jayasinghe et al. [11] used a numerical study to evaluate the response and possible damage to a rock-socketed pile near the soil-rock interface when subjected to ground shock excitation in LS-DYNA. They found that the pile was relatively vulnerable and the soil properties significantly influenced the response of the pile when subjected to blast loading.

Jayasinghe et al. [12] carried out a field test on the pile response to blast-induced ground motion in Singapore. They calculated the structural and geotechnical bearing capacity of the pile using experimental methods and the pile bearing capacity. The results showed that, in a fixed-head pile, the maximum bending moment occurred at the pile head. The free-head pile recorded higher bending moments at the mid-height of the pile and zero bending moment at the pile head due to the absence of restraints at the top. In all cases, the maximum axial force was applied to the pile head.

Ibrahim and Nabil [13] evaluated the risk of a surface blast load on pile foundations. They reported that wall barriers containing expanded polystyrene between the

pile and blast load reduced the blast effect better than other types of wall barriers.

Bakhshandeh Amnieh et al. [14] used numerical and field analysis to investigate the vibrations caused by explosions in oil pipelines. This research records explosion vibrations in the Izeh-Karun 3 main road project using four three-component seismographs. The stresses applied to the oil pipeline were measured using a static analysis of the stress caused by the oil pipeline's internal pressure and a dynamic analysis of the ground vibration. The results showed that the vibrations caused by the blasting operation did not damage the oil pipeline and that the pipelines near the blasting operation were at a safe distance.

The results of research done on the destructive effects of blasts at the ground surface and at depth indicate that it is necessary to take into account their effects and the pressure distribution during the design of structures, especially piles. Explosion research necessitates technical design to mitigate the adverse effects on nearby structures and facilities. The blast impact range and the safe distance at which the pile will avoid structural damage are two critical parameters for the design of a pile under blast loading. Therefore, this study used the coupled Eulerian-Lagrangian method to determine the blast impact range and safe distance for reinforced concrete piles (RC piles) subjected to blast loading. In the present study, the safe distance has been considered to be the minimum distance of an explosive from a pile for which the tension and compression damage values for the concrete are lower than the final tension and compression damage values so that the pile does not experience structural damage.

The blast impact range has been defined as the shortest safe distance to the pile after which the effect of blast loading on the pile becomes negligible. The blast impact range and safe distance are important parameters that can be used to determine the effect of the impact of blast loading on the pile and anticipate aspects of the design that will become necessary to reduce the effects of the blast wave to a suitable range and distance from the pile.

Despite the importance of the effect of blast loading on the design of piles, only a small number of studies have investigated the effect of blast impact range and safe distance under blast loading. The current research investigated the effect of blasts on determining the safe distance and blast impact range for an RC pile using a three-dimensional numerical model in Abacus software.

The results for clayey and sandy soils were compared. To determine the safe distance, 50 to 500 kg of TNT were used beginning at the shortest allowable distance from the pile (1 m) at the ground surface and at depths of 1 to 6 m. The safe distance for each explosive weight was determined so as not to exceed maximum damage to the

RC pile using the tensile and compressive damage values.

The blast impact range also was determined in order to comprehend the influence of the blast length and depth on the RC pile. The blast impact range for Q2/Q1 (ratio of ultimate compressive bearing capacity of pile after the blast to ultimate compressive bearing capacity of pile before the blast) and Ql2/Ql1 (ratio of ultimate lateral bearing capacity of pile after the blast to ultimate lateral bearing capacity of pile before the blast) were investigated for a TNT blast using 50 to 500 kg at the ground surface and at a depth of 6 m from the ground surface.

2. NUMERICAL MODELING

Abaqus version 6.13 uses the FE method and has applications in civil engineering analysis, especially geotechnical engineering. It is also used for analysis of nonlinear dynamic problems, especially blast loading. In Abaqus/Explicit, the effect of blast loading on structures can be analyzed using CEL technique [15].

2. 1. FE Modeling of Soil   A 3D FE model for clayey and sandy soils using Lagrangian elements is presented. The dimensions considered were $30 \times 30 \times 30$ m to prevent boundary effects. The stress-strain response of sandy soil has been modeled using the Drucker-Prager plastic model [10-16]. Because there is no time for drainage to occur under impact blast loading, the soil mass can be considered as a single-phase material under these conditions and total stress analysis can be carried out. In this study, the behavior of clayey soil was simulated using an elasto-plastic Drucker-Prager cap model. This was originally developed to predict the plastic deformation of soil under compression [16,17]. Table 1 lists the characteristics of the sandy soil [10]. The stress-strain curve for Ottawa sand was taken from Chakraborty [10]. Figure 1 shows the curve and stress-strain relationship of Ottawa sand at a strain rate of 1000/s [10]. Table 2 summarized the properties of clayey soil [17].

The mesh for the FE model was generated using eight-node brick elements (C3D8R) with reduced integration and hourglass control. Finer mesh was generated such that the minimum size of the elements near the blast was 10 mm and the maximum size at a distance from the blast was 10 cm [10]. In order to model the soil-pile interaction, the general contact option in Abaqus was used with hard contact in the normal direction and frictional contact in the tangential direction ($\delta=1/3\phi$ [6]).

Boundary conditions constrained the bottom of the model to prevent movement in all directions [10]. In this model, the boundaries were considered to be practically non-reflective [6, 18]. The dimensions of the soil model

were such that the blast wave did not reach the boundaries of the soil space; therefore, it had no effect on the boundaries and returned to the soil space. The vertical, front, and rear boundaries of the soil provided horizontal and rotational fixity to constrain displacement perpendicular to the planes (Ux, Uy, Uz) and rotations (URx = URy = URz = 0), respectively (Figure 2). The FE

TABLE 1. Sandy soil properties [10]

Parameter	Value
modulus of elasticity (E)	28 MPa
Poisson's ratio (ν)	0.2
density (ρ)	1560 kg/m^3
cohesion (d)	0 MPa
angle of internal friction (ϕ)	30°
dilation angle (ψ)	5°

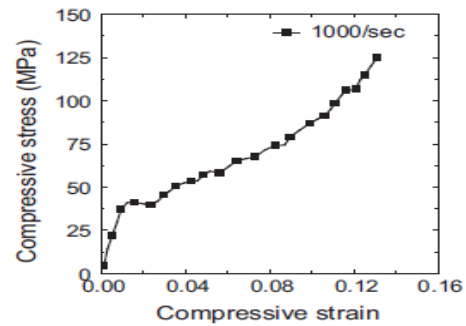**Figure 1.** Stress–strain curve of Ottawa sand at 1000/s strain rate [10]

TABLE 2. Clayey soil properties [17]

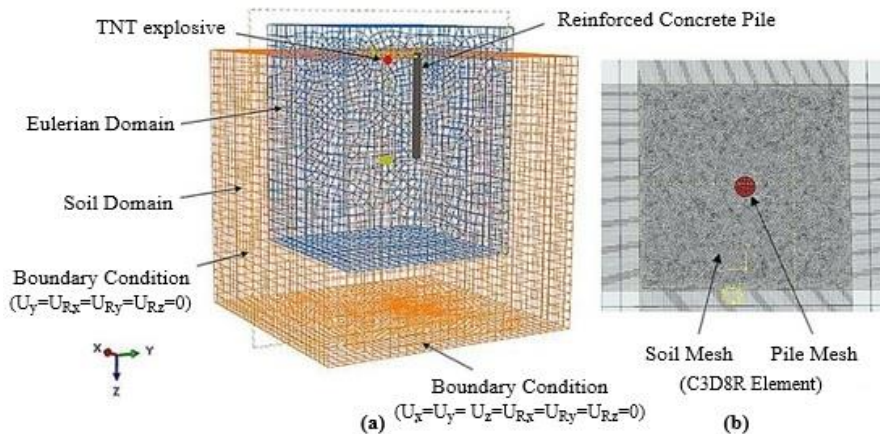| Parameter	Value	
Modulus Of Elasticity (E)	51.7 MPa	
Poisson's Ratio (ν)	0.45	
Density (P)	1920 kg/m^3	
Cohesion (D)	0.036 MPa	
Angle Of Internal Friction (ϕ)	24°	
Cap Eccentricity Parameter (R)	0.3	
Initial Cap Yield Surface Position (ε_v)	0.02	
Transition Surface Radius Parameter (A)	0	
Cap Hardening Behavior	Stress	PVS
	2.75 MPa	0
(Stress- Plastic Volumetric Strain (Pvs))	4.83 MPa	0.02
	5.15 MPa	0.04
	6.20 MPa	0.08

Figure 2. (a) FE model and boundary conditions; (b) soil and pile mesh with types of element

model, mesh, and boundary conditions are shown in Figure 2.

2. 2. FE Modeling of Explosive   The TNT was modeled as a Eulerian element using ABAQUS/CEL. Three-dimensional eight-node continuous elements were used to model the explosives with reduced integration (EC3D8R). The Eulerian elements containing explosive were filled with explosive material and the remainder of the Eulerian grid was a void. In Eulerian analysis, the material is tracked by means of the Eulerian volume fraction (EVF) as it flows through the mesh. The EVF represents the ratio to which each Eulerian element is filled with material; thus, EVF = 1 represents an element that is completely filled with material and EVF = 0 represents a complete void [15]. Eulerian and Lagrangian elements were considered to be in contact (using the general contact option) according to the explosive depth, pile and soil values. In order to avoid reflection of the blast wave into the Eulerian environment, free-flow boundary conditions were considered. The explosive was modeled using the equation of state (JWL). This equation models the pressure created by the blast from a chemical explosive. The JWL equation of state (EOS) is [15]:

$$P = A\left(1 - \frac{\omega\rho}{R_1\rho_0}\right)\exp\left(-R_1\frac{\rho_0}{\rho}\right) + B\left(1 - \frac{\omega\rho}{R_2\rho_0}\right)\exp\left(-R_2\frac{\rho_0}{\rho}\right) + \omega\rho E_m \tag{1}$$

where A, B, R1, R2, and ω are material constants for the TNT. Parameters A and B represent the pressure magnitude, ρ_0 is the explosive density in the solid state, ρ is the current density, and Em is the internal energy per unit of mass. The properties of the explosive for the JWL EOS are shown in Table 3. The explosive mass ranged from 50 to 500 kg of TNT and were modeled as a cubic element at distances of 1 to 4 m in accordance with the safe distance at each explosive mass at the surface and at depths of 1 to 6 m (Figure 3).

TABLE 3. TNT characteristics [10]

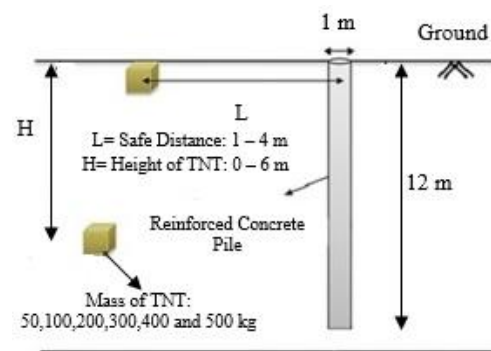| Parameter	Value
density (ρ)	1630 kg/m^3
detonation wave speed (ν)	6930 m/s
A	373800 MPa
B	3747 MPa
ω	0.35
R_1	4.15
R_2	0.9
detonation energy density (E_m)	3680 kJ/kg

Figure 3. Explosive weight and position for modeling

2. 3. FE Modeling of RC Pile   The piles and reinforcements were modeled using Lagrangian elements in ABAQUS/CAE. The diameter and the length of the piles were 1 and 12 m, respectively. The piles were reinforced with 16 tension-compression bars of 25 mm in diameter (16T25). Bars of 10 mm in diameter spaced 100 mm apart (T10@10cm) were used for shear reinforcement of the piles. The concrete and

reinforcements of the piles were modeled using the concrete damage plasticity and Johnson-Cook hardening behavior models, respectively [19]. The properties of the modeled RC piles are shown in Table 4. Stress-strain curves for compression and tension and the damage versus compression and tension strain curves are shown in Figure 4 [19]. The stress-strain behavior of the steel reinforcing bars was defined using the Johnson-Cook (J-C) hardening behavior model. This model is usually used for high strain-rate materials, especially metals. The dynamic yield stress-strain equation of the J-C model with rate dependent strains is [15]:

$$\bar{\sigma} = \left[A + B\,(\bar{\varepsilon}^{pl})^n \right]\left[1 + C\ln\varepsilon^* \right](1 - \hat{\theta}^m) \tag{2}$$

where $\bar{\varepsilon}^{pl}$ is the equivalent plastic strain, ε^* is plastic strain equal to $\varepsilon^* = \dfrac{\dot{\bar{\varepsilon}}^{pl}}{\dot{\varepsilon}_0}$, $\dot{\bar{\varepsilon}}^{pl}$ is the equivalent plastic strain rate, and $\dot{\varepsilon}_0 = 1/s$ is the reference strain rate. A, B, C, m, and n are the constant parameters of the model and

$\hat{\theta}$ is the corresponding temperature. Parameters C and $\dot{\varepsilon}_0$ are related to the dependent strain rate. The properties of the modeled reinforcement bars are shown in Table 5 [10].

TABLE 4. Properties and parameters of RC pile [19]

Parameter	Value
modulus of elasticity (E)	27.4 GPa
poisson's ratio (ν)	0.2
density (ρ)	2400 kg/m³
flow potential eccentricity (ε)	0.1
dilation angle (β)	36°
K_c	0.666
fb0/fc0	1.16

Note: Kc=The ratio of uniaxial tensile deflection stress to uniaxial compressive deflection stress; fb0/fc0=The ratio of biaxial compressive strength of concrete to uniaxial compressive strength.
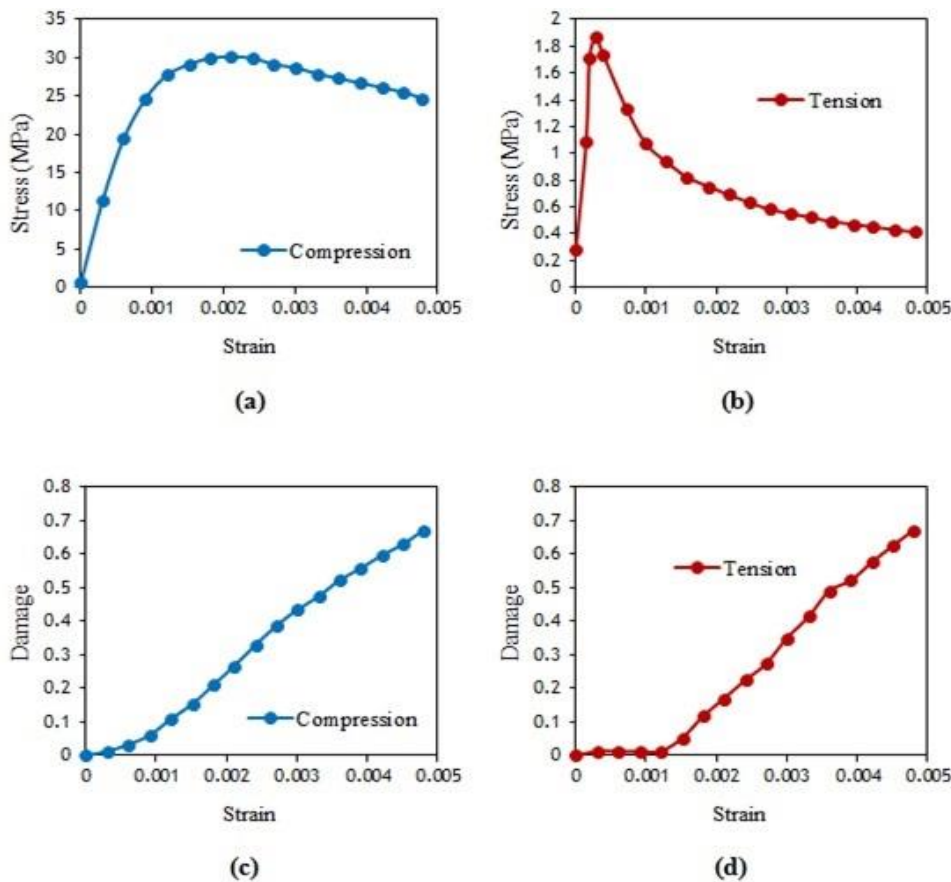

Figure 4. Concrete curves for: (a) compression stress-strain; (b) tension stress-strain; (c) compression damage-strain; (d) tension damage-strain [19]

TABLE 5. Properties and parameters of reinforcement [10]

Parameter		Value
modulus of elasticity (E)		200 GPa
Poisson's ratio (ν)		0.3
density (ρ)		7800 kg/m^3
yield strength (f_s)		350 MPa
hardening parameters of J-C model	A	360 MPa
	B	635 MPa
	n	0.114
	C	0.075

The pile mesh was generated using an eight-node brick element (C3D8R) with reduced integration, hourglass control, and longitudinal and transverse reinforcement using a two-node element (T3D2). The size of the mesh elements was 10 cm for the pile and 1 cm for the reinforcement. The pile-reinforcement interaction was considered using the general contact option and embedment of the reinforcements in the pile was considered using the embedded region option in Abaqus [19]. Figure 5 shows the FE model of the pile and reinforcements.
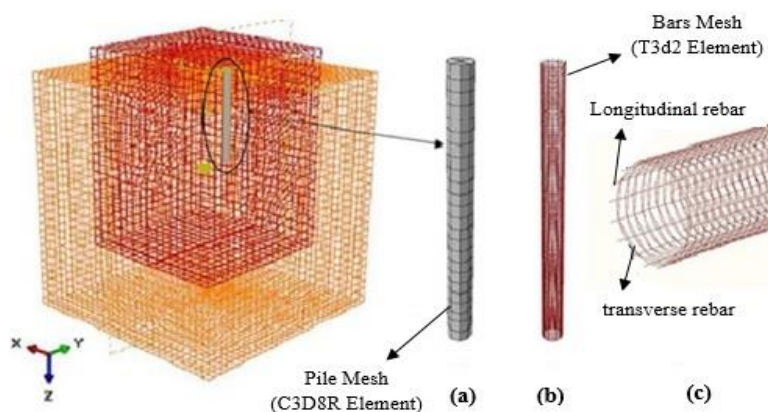
2. 4. Model Analysis   Explicit dynamic analysis was performed using the CEL and central difference integration methods in one step. The CEL method carries out both the Lagrangian and Eulerian methods in Abaqus [18]. In numerical analysis using the CEL method, the Euler materials along the mesh are calculated using EVF. Each Eulerian element represents a percentage that denotes its solidness. The contact between the Eulerian and Lagrangian materials is considered using the general contact option based on the penalty contact method. Lagrangian elements can move along the Eulerian mesh without resistance until they reach an EVF $\neq$ 0 element [6].

The central difference method uses a time difference (Δt) that is smaller than the current time frame. The time difference is represented as $\Delta t \leq l/c$, where l is smallest dimension of the element and c is the speed of sound of the distributed wave in the model. The total time required for analysis was 25 ms; thus, the wave created by the blast was able to spread and transmit throughout the pile. In order to properly distribute the compressive stress wave caused by the blast, artificial bulk viscosity was activated using the quadratic and linear functions and a volumetric strain rate with default values of 1.2 and 0.06 [10].

3. VRIFICATION OF NUMERICAL MODEL

The numerical model was validated in three parts and the results were compared with those from the experimental study by Jayasinghe et al. [7] numerical study using LS-DYNA, and Chakraborty [10] numerical study using Abaqus. Jayasinghe et al. [7] studied an aluminum hollow-pipe pile with a height of 14.3 cm in saturated sandy soil under blast loading in a 70g centrifuge test. The results of displacement along the pile and the maximum stress at different distances from the pile were compared with the results of the present study and the numerical model of Jayasinghe et al. [7]. Figure 6 shows the position of the pile and explosive in Jayasinghe et al. [7] model.

Table 3 shows the properties of the TNT. The sandy soil had a specific gravity of ρsoil = 1937 kg/m^3, elastic modulus of Esoil = 10 MPa, and internal friction angle of ϕ = 31.4° [7]. Figures 7(a) and 7(b), respectively, show displacement along the pile and the maximum soil stress at different distances from the pile from Jayasinghe et al. [7] and the numerical model developed in this study. As seen, the results showed good agreement with those of Jayasinghe et al. [7].

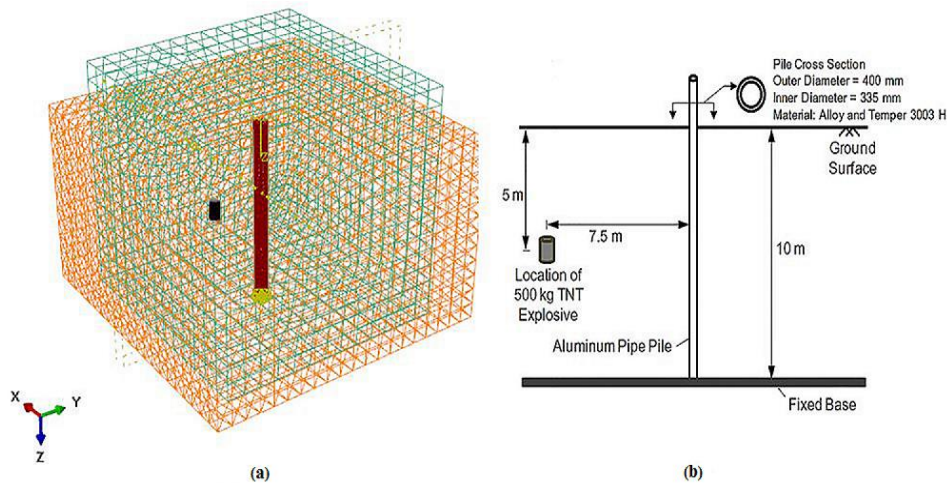**Figure 5.** FE model of: (a) pile mesh; (b) bars mesh; (c) reinforcement

Figure 6. Jayasinghe et al. [7] model: (a) FE modeling for validation; (b) position of pile and explosives in soil
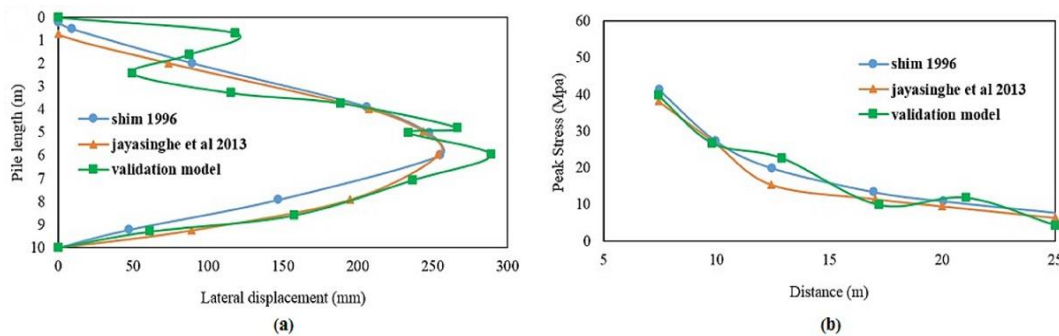

Figure 7. Verification of proposed numerical model using results from experimental model and numerical model [7]: (a) lateral displacement along pile; (b) maximum stress at different distances to the pile

Chakraborty [10] used Abaqus to model two thin steel piles buried in sandy soil exposed to blast loading at a distance of 3 m. A 3D environment of $20 \times 20 \times 20$ m was considered for the soil. The pile was subjected to an axial force of 500 kN. The positions of the piles and explosives is shown in Figure 8. Tables 3 and 5 show the JWL model of the TNT and the properties of the steel pile, respectively. The sandy soil had a specific gravity of specific gravity of ρsoil = 1530 kg/m^3, elastic modulus of Esoil = 28 MPa, internal friction angle of ϕ = 30°, Poisson's coefficient of v = 0.2, and dilation angle of ψ = 5°. The stress-strain response of sandy soil at a strain rate of 1000/s is shown in Figure 1 [10].

Figure 9 compares the maximum lateral displacement of the pile head under blast loading and the results from Chakraborty [10]. As seen, there is an adequate agreement between the results of the current model and Chakraborty [10].

4. RESULTS AND DISCUSSION

4. 1. Determination of Safe Distance of RC Pile Under Blast Loading   In this study, the safe distance

is the minimum distance of an explosive from a pile for which the tension and compression damage values for the concrete are lower than the final tension and compression damage values. At this value, the pile does not experience structural damage. The safe distance of a pile in clayey and sandy soils was determined by comparing the tensile and compressive damage parameters of the RC pile. The concrete damage factor is defined as follows [15]:

$$\sigma = (1-d)E_0\varepsilon \tag{3}$$

where d is the dimensionless factor of concrete damage. This parameter is a criterion for determining the failure area in the concrete. The maximum amount of d denotes complete failure in the concrete. Equations (4) and (5) show the extent of damage to the concrete when exposed to tension and compression, respectively [15]:

$$\sigma_t = (1-d_t)E_0(\varepsilon_t - \varepsilon_t^{pl}) \tag{4}$$

$$\sigma_c = (1-d_c)E_0(\varepsilon_c - \varepsilon_c^{pl}) \tag{5}$$

where subscripts t and c denote tension and compression, respectively, d_t and d_c are the tension and compression
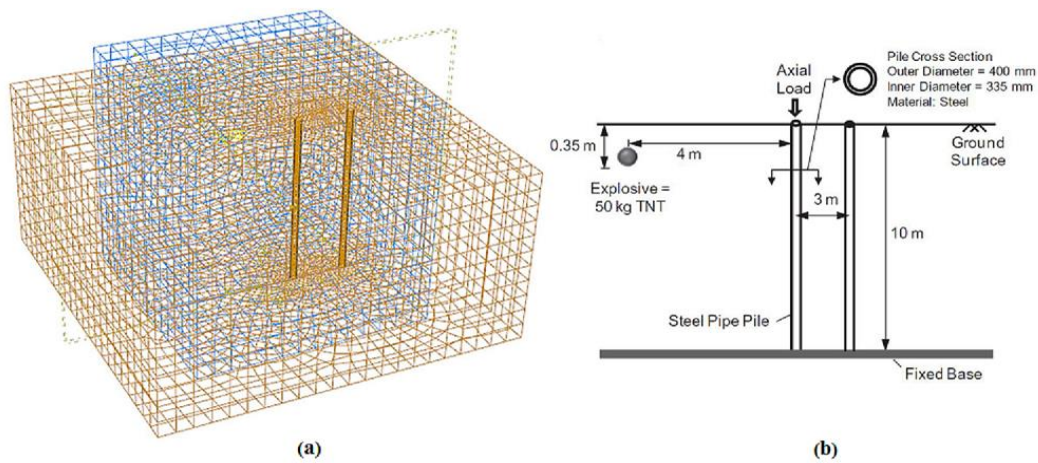
Figure 8. (a) Verified FE model; (b) location of pile and explosive in verified model [10]
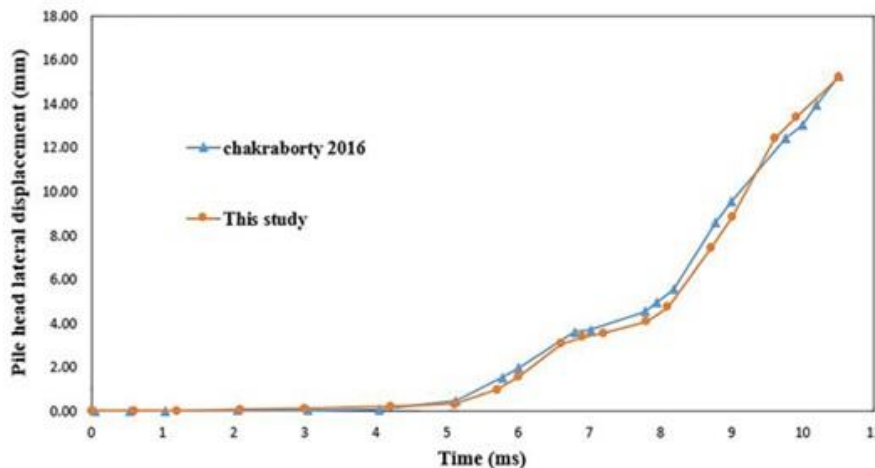

Figure 9. Comparison of pile head lateral displacement results from this study and Chakraborty [10]

damage factors, ε_t and ε_c are the total strains, ε_t^{pl} and ε_c^{pl} are the equivalent plastic strains, and E_0 is the initial (undamaged) elastic stiffness of the material.

A specific concrete damage factor can be defined for each point on the concrete stress-strain curve under compression or tension. Figure 4 shows that the final tension and compression damage values were 0.7437 and 0.7035, respectively. This means that the concrete failed at the final tension and compression damage values and lost effectiveness. This criterion can be used to obtain a safe distance from an explosion to avoid the structural failure of a pile. When the concrete damage factor exceeds the final values, the RC pile will fail; thus, the safe distance can be defined as the distance within which the structure of the pile will not fail under blast loading.

In order to determine the safe distance, initially, 50 kg of TNT was used at the distance nearest to the pile (1 m) and the tension and compression damage values were

obtained. If those values exceeded the maximum concrete damage factor, the distance was increased by 1 m and analysis was repeated until the safe distance was obtained. Analysis was carried out for TNT at the surface of the ground and at depths of 1 to 6 m and for TNT mass of 100, 200, 300, 400 and 500 kg. Figure 10 compares the damage values at safe and unsafe distances for 300 kg of TNT at the surface of the ground in clayey soil. The color red on the pile represents exceedance of the damage value when exposed to tension and compression which resulted in structural failure of the pile. Figures 10(c) and 10(d) do not exceed the damage values for the pile when exposed to tension and compression. Figure 11 shows the tensile and compressive damage values for the RC pile in clayey soil at a distance of 3 m for explosive masses at the surface and at depths of 2, 4 and 6 m.

Figure 11 shows that the tension and compression damage values are below the maximum values (0.7437 and 0.7035, respectively) at a distance of 3 m for all

explosive masses except for 500 kg of TNT. For the 500 kg explosive, these values had reached their final values, and the RC pile broke at this distance.

To obtain a safe distance for 500 kg of TNT, it was placed at a further distance than in the first step (4 m) to reduce the tensile and compressive damage to their ultimate values. Therefore, it can be concluded that a distance of 3 m for all explosive masses below 500 kg is the safe distance. The other tensile and compressive damage values for RC pile at all explosive masses at different depths in clayey soil.

Figure 11 also shows that the damage values decreased as the depth of the blast increased. For example, the tensile damage for 200 kg of TNT at the surface to a depth of 6 m decreased from 0.0755 to 0.0505, a change of 67%. Figure 12 evaluates the tensile and compressive damage to a RC pile in sandy soil at a distance of 3 m for all explosive masses at the surface and at depths of 2, 4, and 6 m.

Figure 12 shows that, unlike in clayey soil, the tension and compression damage in sandy soil was below the

maximum values (0.7437 and 0.7035, respectively) at a distance of 3 m for all explosive masses. The effects of explosive mass and depth of blast on the tensile and compressive damage of the RC pile are similar to those for clayey soil. Comparison of Figures 11 and 12 indicate that the tensile and compressive damage values in sandy soil were lower than in clayey soil under similar conditions.

When a blast occurs, a shock wave propagates through the soil particles. The velocity of the wave depends on the modulus of elasticity (E) and density (ρ) of the soil. In sandy soil, the velocity of the blast wave usually is lower than in clayey soil because of the high values for E and ρ. Therefore, it can be said that sandy soil showed better resistance to blasting damage than did clayey soil.

Table 6 lists the safe distance values for tensile and compressive damage at different distances for masses of 100, 200, 300, 400 and 500 kg of TNT at the surface and at depths of 1 to 6 m. The safe distance for 50 kg of TNT was 1 m, which means that the pile was not damaged at
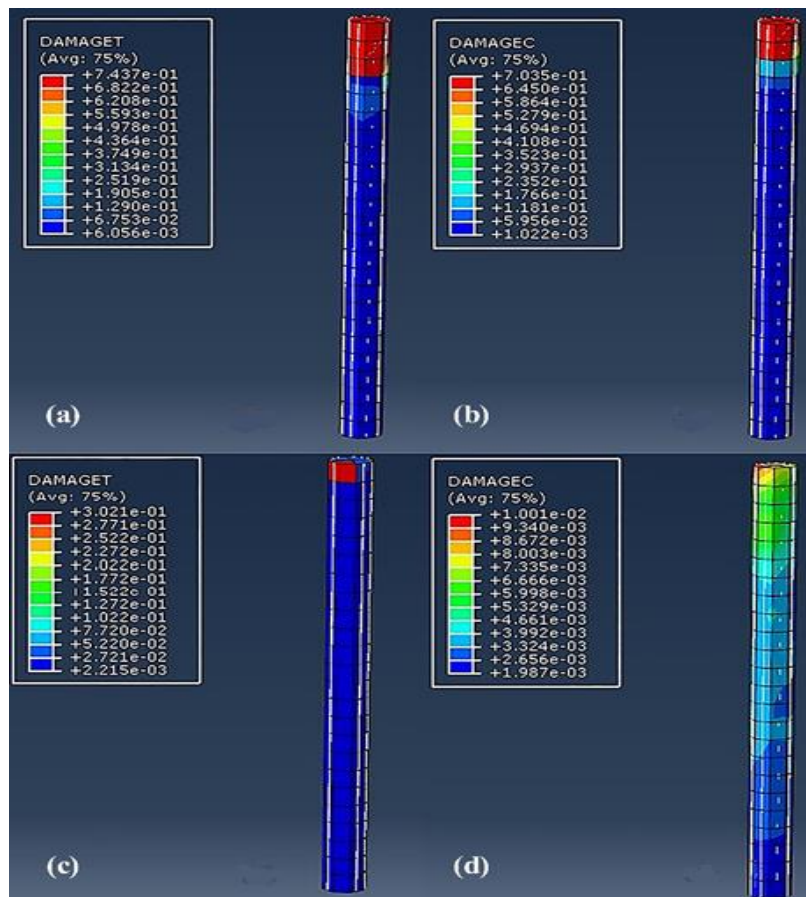

Figure 10. Comparison of damage for 300 kg TNT in clayey soil: (a) tension damage at an unsafe distance of 2 m; (b) compression damage at an unsafe distance of 2 m; (c) tension damage at a safe distance of 3 m; (d) compression damage at a safe distance of 3 m
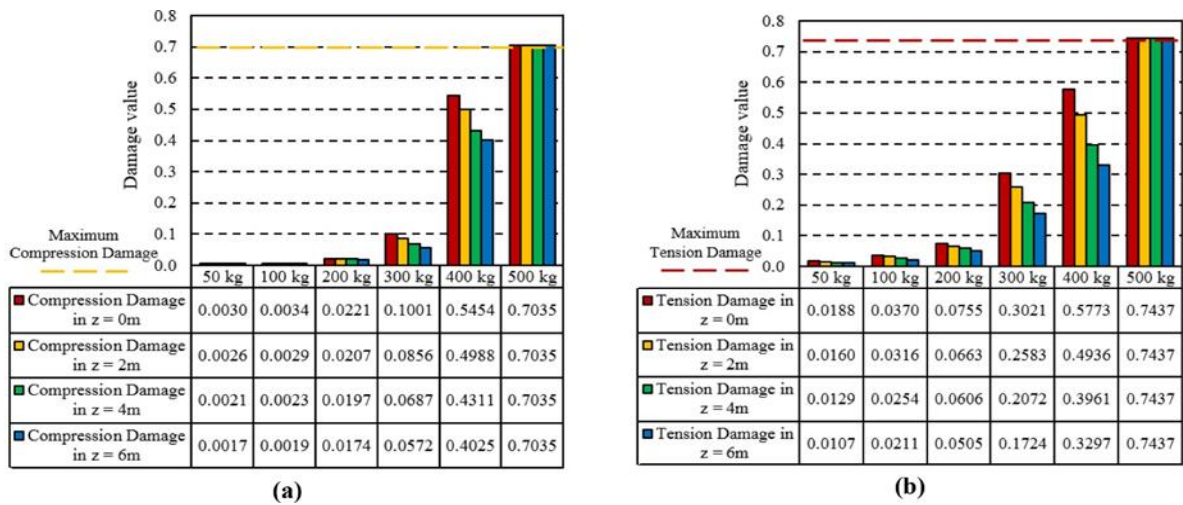
Figure 11. Tension and compression damage in RC piles in clayey soil for all explosive masses at 3 m at the surface and at depths of 2, 4 and 6 m: (a) compression; (b) tension
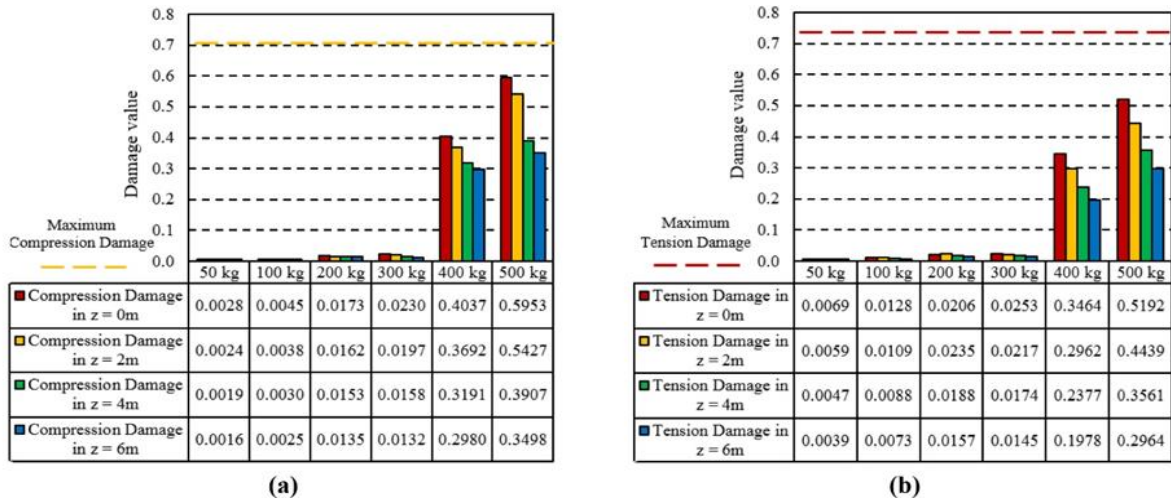

Figure 12. Tension and compression damage in RC piles in sandy soil for all explosive masses at 3 m at the surface and at depths of 2, 4 and 6 m: (a) compression; (b) tension

TABLE 6. Safe distances for all explosive masses at surface and at depths of 1 to 6 m in clayey and sandy soil

Safe distance at all depths (m)		
Mass of TNT (kg)	Clay	Sand
50	1	1
100	2	1
200	2	2
300	3	2
400	3	3
500	4	3

the minimum distance. The safe distance for the RC pile for 100 kg of TNT was 2 m in clayey soil, but under such

conditions, the sandy soil had a safe distance of 1 m, which means that the pile lost efficiency at a distance of 1 m. This suggests that a change in soil type from clay to sand will reduce the safe distance to about 1 m. The reason could be the lower density, lower Poisson's ratio and lower modulus of elasticity of sandy soil compared to clay soil, which better controlled the blast wave and reduced damage [13]. It can be stated that soil type plays a significant role in controlling damage and reducing the safe distance.

An increase in the TNT mass increased the safe distance. For example, the safe distance for 50 kg of TNT was 1 m and for 500 kg TNT was 4 m. The safe distances in clay soil for explosive masses of 100 and 200 kg, as well as for 300 and 400 kg, were the same. Table 6 reveals that the safe distance at different depths were constant in the numerical models and the safe distances

in sandy soil did not change according to depth as they did in the clayey soil. Thus, an increase in explosive depth did not significantly reduce damage (especially tensile damage) at an unsafe distance or reduce the ultimate damage (rupture) in the pile.

Figure 13 shows the tension damage in a pile for 200 kg of TNT at an unsafe distance of 1 m at the surface in both clayey and sandy soil. The damage observed in clayey soil was much greater than that in sandy soil. The damage values in clayey soil exceeded the allowable maximum value (0.7437). In sandy soil, the damage values only reached the boundaries of the maximum value (0.7437). The destruction of the pile shell and reinforcements is shown in Figure 13(a) for clayey soil. It is clear that sandy soil was more effective in controlling damage and damping destructive excitation.

4. 2. Determination of Blast Impact Range in Clayey and Sandy Soil   In this study, the blast impact range has been defined as the nearest safe distance of a pile after which the effect of blast loading on the pile becomes negligible. In order to determine the blast impact range, the nearest safe distance at the surface and at a depth of 6 m was determined for different TNT explosive masses.

This distance then was increased such that Q2/Q1 (the ratio of ultimate bearing capacity of pile after the explosion to ultimate compressive bearing capacity of pile before the explosion) and Ql2/Ql1 (the ratio of ultimate lateral bearing capacity of pile after the explosion to ultimate lateral bearing capacity of pile before the explosion) ratio values approached 1. In other words, the distance was increased until the blast wave no longer had an effect on the pile.

As prepared by Jayasinghe et al. [11] to determine the bearing capacity of piles under blast loading, in the present study, only the geotechnical bearing capacity of the pile was calculated after placing the pile at the safe distance. In order to calculate Q2/Q1 and Ql2/Ql1, the final compression capacity of the pile before the blast was calculated using the Meyerhof method as Q1 [20]. The maximum stress values for skin friction and the tip of the pile after the blast were obtained using the numerical model and were subtracted from the stress values for skin friction and the tip of the pile before the blast. The final compression capacity of the pile (Q2) after the explosion can be calculated as follows:

$$Q_1 = \left[(q_{p1}) \times A\right] + \left[(q_{f1}) \times PL\right] = \left[Q_{p1}\right] + \left[Q_{f1}\right] \tag{6}$$

$$Q_2 = \left[(q_{p1}-q_{p2}) \times A\right] + \left[(q_{f1}-q_{f2}) \times PL\right] = \left[Q_{p2}\right] + \left[Q_{f2}\right] \tag{7}$$

where Qp1 and Qp2 are the bearing capacity of the pile tip before and after the blast, respectively, and Qf1 and Qf2 are the bearing capacity of skin friction before and after the blast, respectively. Variables Qp1 and Qp2 are the maximum vertical stresses at the tip of the pile before and after the blast, respectively, and Qf1 and Qf2 are the maximum vertical stresses on the skin of the pile before and after the blast, respectively. Variables A, P and L are the cross-section, cross-section environment and pile length, respectively.

The lateral bearing capacity of the pile before the blast was calculated using the Broms method as Ql1 [20]. The maximum lateral stress after the explosion was calculated using the numerical model and was subtracted from the corresponding values before the blast. The final lateral bearing capacity of pile after the blast is denoted
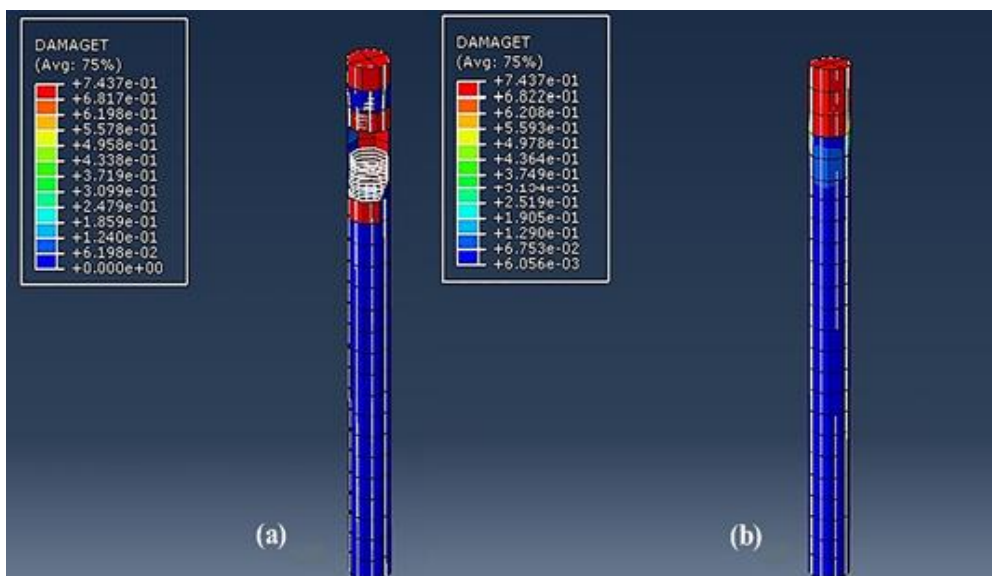

Figure 13. Comparison of tension damage in pile for 200 kg TNT at an unsafe distance of 1 m at the surface in: (a) clayey soil; (b) sandy soil

as Ql2. The blast impact range was obtained for the different explosive masses and is shown in Figure 14. As illustrated, Q2/Q1 increased with an increase in the distance from 50 kg of TNT at the surface in clayey soil. The blast impact range, Q2/Q1, and Ql2/Ql1 at the surface and at 6 m in depth for different explosive weights are presented in Table 7 for clayey and sandy soils. Table 7 summarizes that the blast impact range increased with an increase in the explosive mass. For example, the blast impact range for 500 kg of TNT at the surface was 23 m greater than for 50 kg of TNT. The corresponding difference at a depth of 6 m was only 1 to 3 m because Q2/Q1 increased as the depth increased. It is clear that the blast impact range was greater at the surface of than at depth. Also, the difference with the blast impact range at a higher explosive weight was greater because Q2/Q1 increased at depth compared to the corresponding value at the surface. The ratio of Ql2/Ql1 at a depth of 6 m was same for all explosive masses because the value of Ql2/Ql1 approached 1 for the nearest distance, which means that it did not need to be controlled at greater distances. Therefore, the only parameter that should be measured at depth is Q2/Q1.

Table 7 also shows that the blast impact range increased as the explosive mass increased in both sandy and clayey soils. At 500 kg of TNT in clayey and sandy soils, a difference of 1 to 2 m was detected. This was caused by the ability of the sandy soil to control the blast waves. The blast impact range in clayey soil was 4 to 34 m and in sandy soil was 3 to 32 m. The difference between the blast impact range at a depth of 6 m for the high TNT mass was greater than at the lower mass. The blast impact range in sandy soil at the surface was larger than at depth. In both soil types, the Ql2/Ql1 approached 1 at the nearest distance. This indicates that the only parameter that requires measurement at depth is Q2/Q1. It can be seen in Table 7 that the blast impact range decreased in sandy soil in comparison with clayey soil. This is due to the lower density, lower Poisson's ratio and lower modulus of elasticity of sandy soil compared to clay soil, which caused the generated wave to travel a shorter distance in sandy soil and caused less stress in the soil [13, 20]. Chakraborty [10] also has stated that the most influential soil parameters for blast loading are the internal friction angle and soil density.
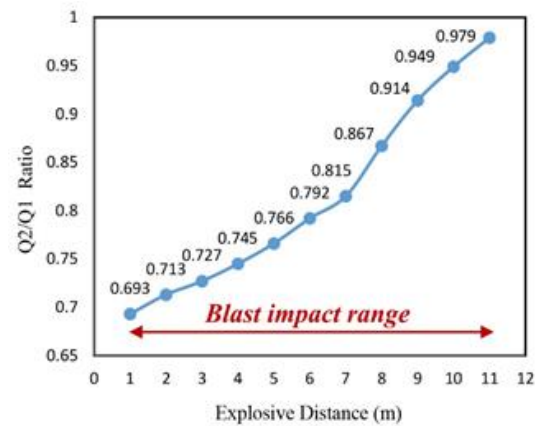

Figure 14. Q2/Q1 vs. distance for 50 kg of TNT at the surface in clayey soil

Table 7. Blast impact range for different explosive mass for blasts at the surface and at depths of 6 m for clayey and sandy soil

Clay					Sand				
Mass of explosive (kg)	Depth of explosive (m)	Blast impact range (m)	Q_2/Q_1 in blast range	Ql_2/Ql_1 in blast range	Mass of explosive (kg)	Depth of explosive (m)	Blast impact range (m)	Q_2/Q_1 in blast range	Ql_2/Ql_1 in blast range
50	0	1-11	0.979–0.693	0.656- 0.980	50	0	1 -9	0.734 -0.982	0.950 -0.993
	6	1-12	0.635-0.960	0.980		6	1-10	0.721 -0.974	0.991
100	0	2-16	0.647- 0.971	0.743- 0.995	100	0	1 -14	0.705 -0.978	0.932 -0.997
	6	2-17	0.514- 0.954	0.985		6	1-15	0.644 -0.963	0.988
200	0	2-20	0.602-0.965	0.576-0.996	200	0	2 -18	0.698 -0.978	0.913 -0.996
	6	2-22	0.417- 0.951	0.934		6	2 -20	0.634 -0.967	0.981
300	0	3-24	0.567- 0.968	0.649- 0.992	300	0	2 -22	0.658 -0.954	0.902 -0.995
	6	3-26	0.329- 0.962	0.955		6	2 -24	0.597 -0.961	0.977
400	0	3-29	0.452- 0.973	0.515- 0.994	400	0	3 -27	0.645 -0.952	0.896 -0.991
	6	3-32	0.290- 0.966	0.929		6	3 -30	0.588 -0.973	0.975
500	0	4-34	0.454- 0.965	0.601- 0.996	500	0	3 -32	0.612 -0.979	0.868 -0.994
	6	4-37	0.303- 0.951	0.962		6	3 -35	0.540 -0.963	0.968

5. CONCLUSION

Explosion research necessitates technical design to mitigate the adverse effects on nearby structures and facilities. The blast impact range and the safe distance at which the pile will avoid structural damage are two critical parameters for the design of a pile under blast loading. Therefore, in this research, 3D dynamic analysis of RC piles subjected to blast loading was numerically conducted in Abaqus. In order to determine the safe distance from the pile, different explosive masses were modeled at the closest possible distance, at the surface, and at different depths. The criteria were the maximum allowable tension and compression damage in the RC pile. In order to determine the blast impact range, the explosive masses were modeled at the closest safe distance from the pile to a distance at which Q2/Q1 and Ql2/Ql1 approached 1. The following conclusions were made:

- An increase in the mass and depth of the explosive increased the blast impact range. For example, in clayey soil, the blast impact range increased about 26 m when subjected to 50 to 500 kg of TNT at the ground surface. For 500 kg of TNT, the blast impact range increased from 34 to 37 m at a depth of 6 m because of the decrease in Q_2/Q_1. In both soil types, explosive loading increased as the depth and mass of the explosive increased.

- The safe distances were shorter for sandy soil than for clayey soil. The safe distance decreased 1 to 2 m when the geotechnical condition changed from clay to sand.

- The tensile and compressive damage and Q_2/Q_1 and Ql_2/Ql_1 of sandy soil were better than for clayey soil. In sandy soil, the maximum tension and compression damage decreased by 65% and 50%, respectively, and Q_2/Q_1 and Ql_2/Ql_1 increased by 25% and 14%, respectively. This indicates that the sandy soil had a higher capacity than clayey soil to resist the effects of blast loading.

- The blast impact range in sandy soil was less than in clayey soil. For example, under 500 kg of TNT at the ground surface, the blast impact range in clayey soil was 4 to 34 m and in the sandy soil was 3 to 32 m.

- If a pile is located at an unsafe distance, structural failure of the pile will occur prior to geotechnical failure. It is important in the design stage to control for structural sufficiency before controlling for the bearing capacity of the pile under blast loading.

- An increase in explosive depth had no significant effect on reducing the compression and tension damage (especially tension damage) at an unsafe distance.

Examining the effects of other parameters and conditions not addressed in this study can be significant and presented as a suggestion for future research. Among others, we can refer to the exploration of the impact of blast loading on piles in soils with different layers in depth, the investigation of the effect of changing soil parameters on the behavior of piles under blast load, and the investigation of the impact of the explosion on piles in saturated and unsaturated soils.

6. REFERENCES

1. Gorashi, S. M. S., Khodaparast, M., Rajabi, A. M., "Evaluation of Dynamic Probing Testing Effect in Hand Excavated Pit on Test Results Using Numerical Modeling", *International Journal of Engineering, Transactions B: Applications,* Vol. 33, No. 8, (2020), 1553-1559. doi: 10.5829/IJE.2020.33.08B.13

2. Gorashi, S. M. S., Khodaparast, M., Khodajooyan. Qomi, M., "Compaction quality control of coarse-grained soils using dynamic penetration test results through correlation with relative compaction percentages", *International Journal of Engineering,* Vol. 36, No. 3, (2023). https://www.ije.ir/article_160375.html

3. Liao, S., Li, W., Fan, Y., Sun, X. and Shi, Z, "Model Test on Lateral Loading Performance of Secant Pile Walls", *Journal of Performance of Constructed Facilities,* Vol. 28, No. 2, (2014), 391-401.https://doi.org/10.1061/(ASCE)CF.1943-5509.0000374

4. Dusenberry, D. O., "Handbook for Blast-Resistant Design of Buildings", *John Wiley & Sons*, USA, 2010.

5. Prasanna, R. and Boominathan, A., "Finite-Element Studies on Factors Influencing the Response of Underground Tunnels Subjected to Internal Explosion", *International Journal of Geomechanics,* Vol. 20, No. 7, (2020), 04020089. https://ascelibrary.org/doi/10.1061/%28ASCE%29GM.1943-5622.0001678

6. Qiu, G., Henke, S. and Grabe, J., "Application of a Coupled Eulerian Lagrangian Approach on Geomechanical Problems Involving Large Deformations", *Computers and Geotechnics* Vol. 38, No. 1, (2011), 30-39. https://doi.org/10.1016/j.compgeo.2010.09.002

7. Jayasinghe, L. B., Thambiratnam, D. P., Perera, N. and Jayasoorya, J. H. A. R., "Computer Simulation of Underground Blast Response of Pile in Saturated Soil", *Computers & Structures,* Vol. 120, (2013), 86-95. https://doi.org/10.1016/j.compstruc.2013.02.016

8. Huang, B., Gao, Q., Wang, J., Jiang, X., Wang, X., Jiang, B. and Wu, W., "Dynamic Analysis of Pile-Soil-Structure Interaction System under Blasting Load", *Applied Mechanics and Materials,* Vol. 638-640, (2014), 433-436. https://doi.org/10.4028/www.scientific.net/AMM.638-640.433

9. Jayasinghe, L. B., Thambiratnam, D. P., Perera, N. and Jayasoorya, J. H. A. R., "Blast Response of Reinforced Concrete Pile Using Coupled Computer Simulation techniques", *Computers & Structures,* Vol. 135, (2014), 40-49. https://www.sciencedirect.com/science/article/abs/pii/S0045794914000285

10. Chakraborty, T., "Analysis of Hollow Steel Piles Subjected to Buried Blast Loading", *Computers and Geotechnics,* Vol. 78, (2016), 194-202. https://doi.org/10.1016/j.compgeo.2016.05.015

11. Jayasinghe, L. B., Zhou, H. Y., Goh, A. T. C., Zhao, Z. Y. and Gui, Y. L., "Pile Response Subjected to Rock Blasting Induced Ground Vibration Near Soil-Rock Interface", *Computers and*

Geotechnics, Vol. 82, (2017), 1-15. https://doi.org/10.1016/j.compgeo.2016.09.015

12. Jayasinghe, L. B., Zhao, Z. Y., Goh, A. T. C., Zhao, H. Y., Gui, Y. L. and Tao, M., "A Field Study on Pile Response to Blast-Induced Ground Motion", *Soil Dynamics and Earthquake Engineering,* Vol. 114, (2018), 568-575. https://doi.org/10.1016/j.soildyn.2018.08.008

13. Ibrahim, Y. E. H. and Nabil, M., "Risk of Surface Blast Load on Pile Foundations", *Magazine of Civil Engineering,* Vol. 90, No. 6, (2019), 47-61. https://engstroy.spbstu.ru/en/article/2019.90.5/

14. Bakhshandeh. Amnieh, H., Mahdi. Mirabedi, S. M., Rahmanpour, M., Jafari, V., "A Study of Blast-induced Vibration on Oil Pipelines based on Numerical and Field Analysis", *International Journal of Engineering, Transactions C: Aspects,* Vol. 34, No. 9, (2021), 2116-2123. doi: 10.5829/IJE.2021.34.09C.09

15. Abaqus, ABAQUS/Explicit User's guide, Version 6.13, Providence, Dassault Systèmes Simulia Corp, Inc, USA, (2013).

16. Helwany, S., "Applied Soil Mechanics: with Abaqus Applications", *John Wiley & Sons*, USA, 2007.

17. Nagy, N., Mohamed, M. and Boot, J. C., "Nonlinear Numerical Modelling for The Effects of Surface Explosions on Buried Reinforced Concrete Structures", *Geomechanics and Engineering,* Vol. 2, No. 1, (2010), 1-18. https://doi.org/10.12989/gae.2010.2.1.001

18. Abaqus, ABAQUS/Explicit User's manuals, Version 6.13, Providence, Dassault Systèmes Simulia Corp, Inc, USA, (2013).

19. Tiwari, R., Chakraborty, T., and Matsagar, V., "Dynamic Analysis of Twin Tunnels Subjected to Internal Blast Loading", *Advances in Structural Engineering,* Vol. 6, No. 30, (2015), 343-354. https://doi.org/10.1007/978-81-322-2190-6_30

20. Tomlinson, M., Woodward, J., "Pile Design and Construction Practice", *Taylor & Francis Group*, UK, 2014.

Persian Abstract

چکیده

شمع‌ها بارهای سازه‌ای را به لایه‌های سخت خاک یا سنگ منتقل می‌کنند. بنابراین هرگونه آسیب به شمع‌ها می‌تواند عواقب جبران ناپذیری داشته باشد. یک انفجار سطحی می‌تواند یک شوک زمین ایجاد کند که انرژی انفجار را در امتداد سطح و در اعماق منتقل می‌کند. بررسی اثرات انفجار نیازمند طراحی فنی برای کنترل اثرات نامطلوب آن بر سازه‌ها و تاسیسات مجاور است. از جمله پارامترهای اساسی برای طراحی یک شمع تحت بارگذاری انفجار، محدوده تاثیر انفجار و فاصله ایمن است که در آن از آسیب سازه‌ای شمع جلوگیری می‌شود. لذا در این تحقیق مطالعه عددی شمع‌های بتن مسلح تحت بارگذاری انفجار با استفاده از روش کوپل اویلری–لاگرانژی جهت تعیین محدوده تاثیر انفجار و فاصله ایمن شمع‌ها انجام شد. نتایج برای خاک‌های رسی و ماسه‌ای نشان داد که افزایش عمق انفجار علیرغم کاهش آسیب فشاری و کششی به شمع، تأثیر قابل ملاحظه‌ای بر فاصله ایمن نداشت. افزایش جرم و عمق انفجار ظرفیت باربری فشاری نهایی شمع را کاهش و محدوده تاثیر انفجار را افزایش داد. خاک ماسه‌ای بهتر از خاک رسی در برابر بار انفجار عمل کرد. نتایج این پژوهش می‌تواند در پروژه‌های مختلف از جمله برای سازه‌های با اهمیت زیاد که در مجاورت خطوط انتقال گاز قرار گرفته و یا ممکن است در معرض حملات تروریستی قرار گیرند، استفاده شود.